Comparative Study for EAF's Reactive Energy Compensation Methods and Power Factor Improvement

DEACONU SORIN IOAN[1] , POPA GABRIEL NICOLAE[1] , TIHOMIR LATINOVIC[2]
[1] Department of Electrotechnical Engineering and Industrial Informatics,
"Politechnica" University of Timisoara
Revolutiei str., no. 5, Hunedoara, 331128
ROMANIA
[2] Department of Robotics, University of Banja Luka, Bosnia and Hertegovina
sorin.deaconu@fih.upt.ro, http://www.fih.upt.ro

Abstract: - In this paper is analyzing the current operating conditions of one electric arc furnace (EAF) in order to evaluate the best option to solve the energy consumption problem. Experimental results show that EAFs represent a substantial source of electric disturbances, such as voltage fluctuations, flicker, harmonics, and unbalance between phases. Improvement of the energetic performances of an EAF imposes a careful technical and economical analysis. The possible compensation solutions include passive filter, SVC (static var compensator) and STATCOM (static synchronous compensator).Finally, the guideline for compensator selection and performance estimation is obtained.

Key-Words: - Electric Arc Furnace, Flicker, Power Factor, Harmonic Analysis, Reactive Compensator, Improvement

1 Introduction

A great percent of the world production is provided by large capacity electric arc furnaces (EAF). EAF are placed among the biggest polluters of air, soil, water and electric supply grids. Also the energy consumption is significant [1].

The ability to precisely control the temperature and chemistry of the batch make EAFs an ideal choice for producing high-grade steel for the recycling of scrap. Of the steel made today 36% is produced by the EAF route and this share will increase to 50% by 2030 [2].

The EAF has been studied for many years, but it is still difficult to complete representation of such load and its impact on the power system.

Due to the dynamic behavior of the arc during the melting process, an EAF is a major source of perturbations on a high voltage grid with a low short-circuits capacity. The perturbations are of random nature and encompass a frequency range from DC to a few hundreds of Hz.

The beginning of an EAF heating cycle involves introducing the electrodes into the scrap steel to start the melting process. The arc established at this time is very unstable, and the electrodes are short-circuited by the scrap metal at times. During the melting period the arc length changes as a result of the electromagnetic force and the continuous movement of the molten pool. The power into the furnace is mostly reactive, with large swings in furnace current between short-circuit levels to near zero. This can cause severe voltage flicker in the connected utility power system [3].

In contrast to other types of loads which are usually operated by voltage steps, EAFs produce random flicker which cannot be easily calculated with standard curves and methods [4].

Voltage fluctuations in electric power system may cause significant illumination changes in lighting equipment [5]. This unsteadiness of visual sensation, witch is induced by a light stimulus whose luminance or spectral distribution fluctuates with time, is called flicker. When flicker exceeds some certain threshold, the phenomenon becomes annoying and the annoyance very rapidly depending on the fluctuation's amplitudes [6].

The electrical design of a modern arc furnace installation involves a study encompassing the complete power circuit from the utility company's generators to the arcs in the furnace. The study also entails the selection of suitable circuit components as required to put the desired power into the furnace at optimum conditions and to restrict cyclic voltage changes (flicker) to acceptable limits at some designated point in the power system and correct power factor as required. Occasionally, someone will suggest the use of a higher impedance step-down transformer between

the utility system and the high-voltage furnace bus to reduce the surges on the utility system. This reasoning is completely erroneous, as the furnace builder would simply select a higher no-load furnace voltage to maintain the desired arc characteristics. This, if anything, would produce slightly larger swings between no-load and short circuit [7] ,[8].

The electric arc is a nonlinear element. For study the behavior of the systems containing an electric arc it must use techniques to model the nonlinearity of the electric arc. The electric arc furnace (EAF) is a source of harmonic currents and reactive power in electrical power system because the electric arc's nonlinearity. EAF represent also an unbalance load. In order to improve the functioning of the EAF it can be used harmonic filters reactive power compensation installation and load balancing [9].

For simulation it was use an electric arc model, depending on the nonlinearity of the electric arc. The modeling approach adopted in the paper is graphical, as opposed to mathematical models embedded in code using a high-level computer language.

Neuronal networks prove to be useful for solving some difficult problems, such as: estimating, identifying, predicting, and controlling or for complex optimization. Because each operation should be independent – we refer to all components of the system – connection patterns may work in parallel. The way data is memorized and processed differentiate the artificial neuronal networks from all classic software. The classic software follows the instructions according to a pre-defined sequential order. Due to their features, which enable them solve any difficult problem, based on a large number of examples, connection systems we use for different occasions: shape acknowledge systems or signals, systems for controlling complex processes [10].

2 The Power Quality Analysis

The criteria of quantitative analysis of power quality are [8]:

− The power factor

$$K_P = P / S = P / \sqrt{P^2 + Q^2 + D^2} \,. \quad (1)$$

− The reactive factor and respectively the deforming factor

$$K_Q = Q / S \,, \quad (2)$$

$$K_D = P / \sqrt{P^2 + Q^2} \,, \quad (3)$$

where P is active power, S is apparent power, Q is reactive power and D is distorting power.

− The total harmonic distortion for current and voltage (%)

$$THDI = \sqrt{\sum_{k=2}^{40} \left(\frac{I_k}{I_1} \right)^2} \cdot 100, \quad THDU = \sqrt{\sum_{k=2}^{40} \left(\frac{U_k}{U_1} \right)^2} \cdot 100, \quad (4)$$

where U_1, I_1 are the rms values for voltage and current on the fundamental and U_k, I_k the effective values for current and voltage on the k-th harmonic order.

− The negative non-symmetry factors for voltage and current (%):

$$k_U^- = U^- / U^+ \cdot 100, \qquad k_I^- = I^- / I^+ \cdot 100 \,. \quad (5)$$

− The zero non-symmetry factors for voltage and current (%):

$$k_U^0 = U^0 / U^+ \cdot 100, \qquad k_I^0 = I^0 / I^+ \cdot 100 \,, \quad (6)$$

where U^- and I^- are the inverse sequences components, U^+ and I^+ are the direct sequences components and U^0 and I^0 are the homopolar components of voltages and currents.

The electrode consumption is calculated, as follows:

$$C_S = \frac{0.065 \cdot I_{ave}^2 \cdot t_n}{G} + 5 \cdot 10^{-5} \cdot d \cdot h \cdot \frac{t_t}{G} \quad , \quad (7)$$

where: C_S is specific electrode consumption $\left(\frac{kg}{t} \right)$, I_{ave} average secondary current (kA), G gross weigh charge (t), d electrode diameter (mm), h distance between electrodes (mm), t_n net time per charge (hours), t_t total heat time (hours).

The flicker problem is analyzed in accordance to the percentage decrease in voltage at the point of common coupling (PCC) when furnace goes from open circuit condition to short circuit on all three phases, expressed as short circuit voltage depression (SCVD) with:

$$SCVD = \frac{V_{OC} - V_{SC}}{V_{OC}} \cdot 100 \,, \quad (8)$$

where V_{OC} is voltage at open circuit conditions (V) and V_{SC} voltage at short circuit condition (V).

In the following equations: I_{pp} is the positive peak of the line current; I_{pm} is the negative peak of the line current; V_{pp} is the positive peak of the phase voltage; V_{pm} is the negative peak of the phase voltage; i represents the phase (i = 1, 2, 3); N represents the number of the samples per period (between two consecutive zeros).

Mathematical formulae used to compute the peak factors for current and phase voltage are:

$$I_{CF\,i} = \frac{max\left(I_{pp\ i}, I_{pm\ i}\right)}{\sqrt{\frac{1}{N} \cdot \sum_{k=0}^{N-1} \left(I_{(k)i}\right)^2}} \,, \quad (9)$$

$$V_{CF\,i} = \frac{max\left(V_{pp\ i}, V_{pm\ i}\right)}{\sqrt{\frac{1}{N} \cdot \sum_{n=0}^{N-1} \left(V_{(n)_i}\right)^2}} \,. \quad (10)$$

3 Solutions for flicker mitigation

One definition of flicker is "Impression of unsteadiness of visual sensation induced by a light stimulus whose luminance or spectral distribution fluctuates with time" [11]. This means the perception of light flicker is a physiological process. Over the past years numerous studies have been conducted in order to understand the mechanisms behind the flicker phenomenon. There are at least three different mechanisms influencing the light flicker perception by a human. These are:

- The characteristics of the light source;
- The frequency response of the eye-brain of a human;
- The time constant of the eye-brain.

From the power flow point of view, the basic principle of the flicker mitigation solution can be simply explained as shown in the Fig. 1. The power consumed by EAF can be regarded as a constant power (P_C, Q_C) plus a fluctuating power (ΔP_f, ΔQ_f). Generally, P_C affects the angle stability, Q_C affects the bus voltage profile, voltage stability, and load power factor. ΔP_f is mainly related to the fluctuations of bus voltage angle while ΔQ_f is mainly related to the fluctuations of bus voltage magnitude [12]. An obvious total solution to solve the EAF power quality issue is to compensate Q_C by amounts ΔP_f and ΔQ_f so that the source only supplies constant P_C at unity power factor and so that the source bus voltage has a constant magnitude and angle. However, a total solution is not necessary and a cost-effective alternative is to provide compensation by supplying ΔP_f and ΔQ_f only in the troublesome frequency range, that is, the EAF flicker frequency range of 1Hz ~ 20 Hz [12].

How to economically and efficiently mitigate EAF flicker is consistently a tough issue for utility and industry professionals. The basic methodology for flicker mitigation can be categorized into three types [13]:

- passive filters, which can be either series or shunt;
- series active compensator, such as the series impedance regulation;
- shunt active compensator, such as SVC (static var compensator) and STATCOM (static synchronous compensator).

Though passive filters are simple, reliable, low-cost and highly efficient, it is difficult to design for a stiff system, time-consuming for tuning, easy to induce resonance, and susceptible to system impedance variations [13].

Although the increasing series reactance can mitigate the flicker, it results in the voltage reduction and therefore decreases EAF productivity. Moreover, it is also expensive and laborious to control upstream transformer reactance or series reactor in the firmer deregulation power system [13].

SVC can improve system power quality, and also increase EAF productivity and provide additional economic benefits. However, it cannot react to the fast-varying flicker very well with the inherent limit of relatively low bandwidth and hence its dynamic performance for flicker mitigation is limited. The STATCOM is based on high frequency switching voltage-source converter (VSC). While SVC performs as a controlled reactive admittance, STATCOM functions as a synchronous voltage source.

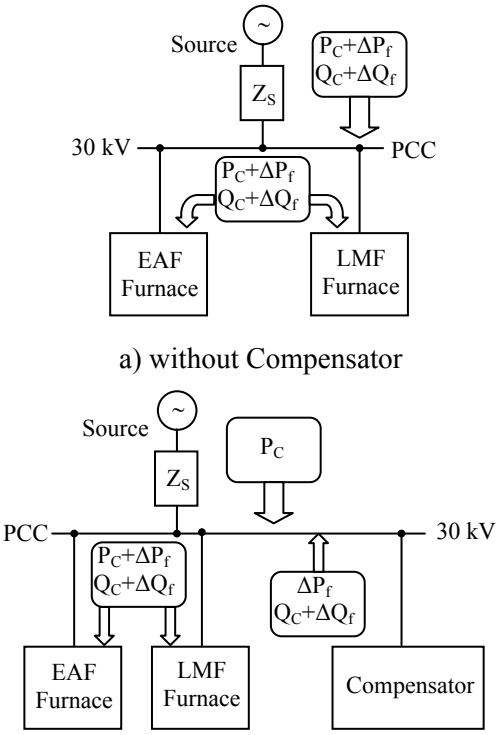

Fig. 1 Arc Furnace Compensation Block Diagram

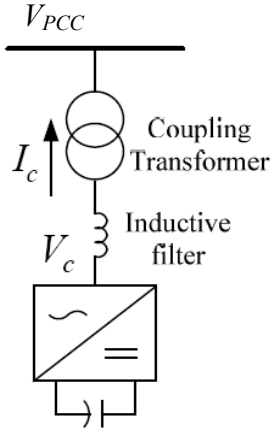

Fig. 2 STATCOM basic structure

The Cascade-Multilevel Converter (CMC), which is constructed with identical H-bridge Voltage Source Converters (VSCs), is the most feasible topology for a shunt-link compensator application because of its compact structure, modularity, fast response and clean power quality. Considering the challenging requirements of an Energy Storage Systems (ESS) to meet a large power density, a small energy density, and fast deep charge and discharge capability, an Ultracapacitor (UC) is a superior energy storage unit for EAF applications [12].

Conventionally, STATCOM is composed of one inverter with energy storing capacitor on its dc side, inductances and a coupling transformer on its ac side, which is connected in parallel with the system at the point of common coupling (PCC), as shown in Fig.2, the fundamental principle of STATCOM is the generation of a controllable ac voltage source by a voltage source inverter (VSI) [14].

In recent years, multilevel voltage source inverter has gained much attention. The inverter can use a number of techniques to construct high-quality ac waveforms from several switched dc sources, so it is possible to achieve high-voltage low-distortion ac waveforms, which result in lower harmonic generation, smaller reactor size, and eliminating bulky and costly transformer. There are three well-established topologies of multilevel inverter: neutral point clamped, flying capacitor and CHB converter configuration [14].

A seven level single phase CHB multilevel converter is illustrated in Fig.3. One of the main disadvantages of the CHB-based STATCOM is the voltage imbalance between the multiple floating dc capacitors, unequal conducting and switching losses produced by power switching devices, as well as resolution issues inherent in the control circuit, may bring voltage imbalance to the dc capacitors [14].

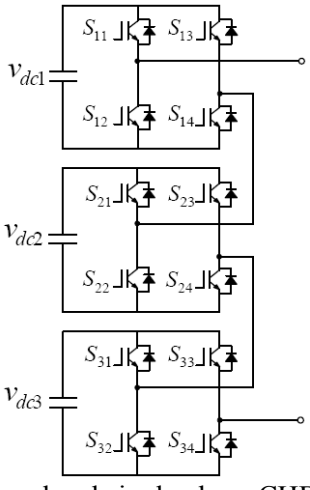

Fig. 3 A seven level single phase CHB multilevel converter

Both current and voltage-fed inverters generate harmonics back into power lines in the process of rectifying AC to DC. Harmonics flowing in the network causing additional losses and decreasing the equipments lifetime. Also, the harmonics can interfere with control, communication or protection equipments. In addition to the harmonics that are normally expected from different pulse rectifiers, large furnaces operating at a few hundred hertz can generate interharmonics. Interharmonics can overload power system capacitors, introduce noise into transformers, cause lights to flicker, instigate UPS alarms, and trip adjustable-speed drives. High-frequency systems, which operate at greater than 3 kHz are relatively small and limited to special applications. Electromagnetic pollution produced by the operation of these equipments is small [15].

4 System description and experimental investigation

A one-line diagram of the studied system is shown in Fig. 4. The 75 MVA arc furnace is supplied from a local feeder with a 30 kV bus voltage. The local feeder is in turn supplied from a 220 kV transmission line through a 160 MVA, 220/30 kV transformer. The compensator is planned to be installed on the EAF 30 kV bus (PCC) as this is the most effective location, primarily because of voltage magnitude considerations.

Typically, the EAF's major processes are melting (early melt) and the refining (late melt). During these two processes, the EAF's electrodes are short-circuited to scrap metal and consume time-varying power, which is mainly dependent on arc lengths.

In table I are given the characteristics of the sources and of the T_1, T_2, T_3 and T_4 transformers [16].

This research theme was required by the beneficiary because the costs with the reactive energy are very high. In addition, if the reactive energy consumption is compensated, the power factor increases and the furnace has available a higher power for melting, the average heat time being reduced.

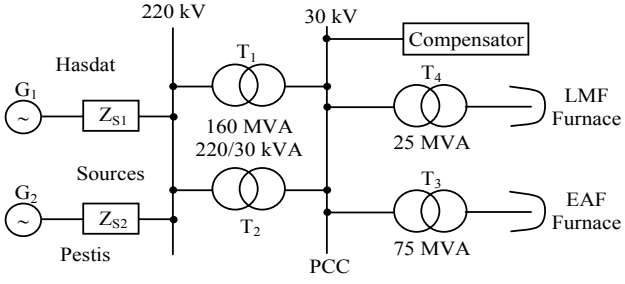

Fig. 4 One-line diagram of the system

Table I

Concept	Unit		
Source		Pestis	Hasdat
Reference Voltage	kV	220	220
Frequency	Hz	50	50
Reactance	PU	0.02088	0.01871
Resistance	PU	0.00182	0.00163
Impedance	PU	0.02096	0.01879
X/R		11.5	11.5
Step Down Transformer		T_1	T_2
Impedance	%Z	16.38	16.38
Capacity	MVA	160	160
Reference Voltage	kV	239.2	239.2
HV Tap	kV	239.2	239.2
LV Tap	kV	33	33
X/R		19.91	19.91
Impedance	Ohm	58.576	58.576
Source+Furnace Transformer		T_3	T_4
Secondary Voltage	V	750	690.7
Capacity	MVA	75	25
X/R		17.358	21.167
Impedance	PU	0.0365	0.0511
HV Connection		Delta	Delta/Wye
LV Connection		Delta/Wye	Delta/Delta

In table II are presented the additional costs with the reactive energy in 2008.

Taking into account the total values paid for the reactive energy in one year (827700.29 Euro at a power factor of 92%) and the system operator intends to increase the value of the neutral power factor to 94% (for which would be paid 944855.72 Euro) is imposing the urgent adaption of a solution and its practical implementation.

In table III are presented the main production indicators obtained in 2008.

To compensate the multiple EAF in Operation it is applied the Jenkin Method as follows:

$$S_{eq} = S_{Largest} \times \sqrt{M_1 + c\sqrt{M_2}}\ , \tag{11}$$

$$M_i = K_i \cdot \left[\sum_{EAF=1}^{N} \left(\frac{S_{EAF}^{(2\times i)}}{S_{Largest}} \right) \right], \tag{12}$$

$$b = \frac{M_3^2}{M_2^2}, \tag{13}$$

where S_{eq} – is equivalent size of EAF, [MVA];

$S_{Largest}$ - size of the largest EAF, [MVA];

S_{EAF} - size of each EAF, [MVA];

$M_{1,2,3}$ - statistical moments;

$K_{1,2,3}$ - weighing factors;

N - total EAF's in the system;

c - stretch factor (from chart of Guide Number);

b - Guide Number.

For our configuration $S_{Largest} = 75$ MVA and $S_{EAF\ LMF} = 25$MVA, results

$$S_{eq} = 75.84MVA\,. \tag{14}$$

In order to propose a solution for improving the operation and a compensation solution, there were made experimental measurements, a part of the results being presented in the next figures [16].

In fig. 5 is presented the variation form of the line voltages on the bar of 30 kV. Against the nominal value takes place a variation comprised within ±10%. The more pronounced variations can be observed in the melting phase (early melt). There are significant differences between voltages caused by the working mode of the electrodes and their operation regime [17].

Table II

2008	Cumulated Active Energy [MWh]	Cumulated Reactive Energy [MVArh]	Power factor	Excess of Reactive Energy [MVArh]		Billing [Euro]	
Month				PF = 92%	PF = 94%	PF = 92%	PF = 94%
1	24949.91	22194.96	74.72	11.533.34	13139.35	76466.37	86865.71
2	47714.63	40754.13	77.51	8861.44	10296.68	58584	68072.53
3	71788.99	63712.55	72.37	12702.78	14220.59	83979.51	94013.91
4	97815.20	97613.33	73.65	12813.66	14454.52	84712.54	95560.49
5	124438.45	110151.20	76.32	11196.41	12874.91	74020.72	85117.52
6	142990.92	125643.81	76.76	7589.28	8758.95	50173.62	57906.45
7	164626.42	144399.16	75.56	9538.66	10902.71	63061.20	72079.06
8	183980.63	160763.03	76.36	8119	9339.22	53675.65	61742.66
9	204818.46	178251.05	76.60	8611	9924.89	56929.23	65614.61
10	232389.63	202178.96	75.52	12182.64	13920.91	80540.80	92032.70
11	254595.56	221729.83	75.05	10091.31	11491.32	66714.81	75970.43
12	277698.01	243625.15	74.11	11925.65	13595.24	78841.84	89879.65
Total				125198.17	142919.29	827700.29	944855.72

Table III

		Month - 2008												
EAF Concept	Unit	1	2	3	4	5	6	7	8	9	10	11	12	Average
Production (Finished Product)	ton	37,020	32,080	33,719	38,125	39,614	25,235	28,736	25,641	28,213	38,535	30,686	28,436	32,170
Heats		341.0	299	314	360	369	247	281	251	266	361	287	269	304
Heat Production (Finished)	Ton/Heat	108.6	107.3	107.4	105.9	107.4	102.2	102.3	102.2	106.1	106.7	106.9	105.7	105.7
Scrap Charged	Ton/Heat	129.94	125.71	125.26	125.40	125.81	126.03	127.23	125.94	125.84	124.89	124.3	124.5	125.9
Yield (Finished Product)	%	0.835	0.853	0.857	0.845	0.853	0.811	0.804	0.811	0.843	0.855	0.860	0.849	0.840
Tap-to-Tap	min/Heat	120.1	127.2	125.2	110.7	111.0	124.9	128.1	129.1	120.2	115.4	126.6	122.4	121.7
Delays	min/Heat	60.1	63.7	66.7	54.2	53.6	64.1	66.2	68.6	58.8	52.8	63.6	61.6	61.2
Melting Power On Time	min/Heat	60.0	63.5	58.5	56.5	57.4	60.8	61.9	60.5	61.4	62.7	63.0	60.8	60.6
Energy Consumption EAF	kWh/Ton	578.3	599.4	596.5	591.0	577.6	635.9	642.1	642.6	620.7	614.1	609.0	607.1	609.5
Electrode Consumption EAF	Kg/Ton	2.64	2.68	2.59	2.69	2.51	2.18	2.78	2.93	3.41	2.39	2.97	2.41	2.68
Gas Consumption-heat ladle	Nm3/Ton	9.6	14.6	14.8	12.2	10.5	15.3	14.1	14.7	13.6	9.2	10.9	14.1	12.8
Oxygen Consumption	Nm3/Ton	16.8	17.0	34.6	34.3	33.7	29.1	41.8	33.5	37.6	26.3	25.7	23.1	29.5
Carbon EAF Charge	kg/Ton	5.1	10.1	11.0	13.5	12.7	9.8	10.7	11.8	8.2	10.8	9.7	13.3	10.6

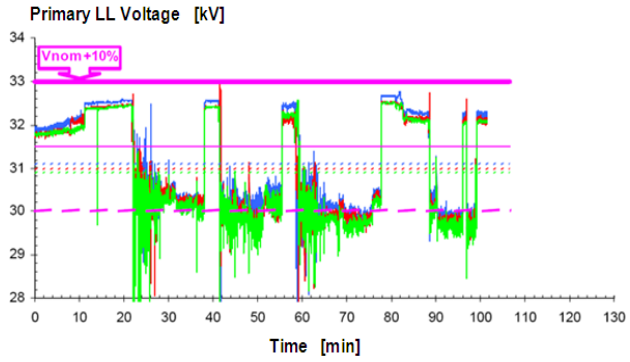

Fig. 5 Line voltages in the EAF transformer's primary

The current's variation form in the EAF transformer's secondary and the arc's stability are given in fig. 6.

One can notice that the great current variations determine a pronounced instability of the electric arc. The variation of the active and reactive power depending on the current in secondary during the melting itself (early melt) is presented in fig. 7 and 8. The average active power is around 62 MW and the average reactive power 47 MVAr.

The dependency of the power factor on the current in secondary for the two melting phases (early melt and late melt) is given in fig. 9 and 10.

In the first case (fig. 9) results an average value of 78% and in the second case (fig. 10) of 84%.

The measurements were made during more heats, and the presented results were selected from the most suggestive ones [16].

In fig. 7, 8, 9 (early melt) the current's variation field is large (40÷86 kA) and in fig. 10 (late melt) this field is restraining (56÷60 kA). Due to the smaller current variations and increased stability in operation (fig. 6), takes place a reduction of the reactive energy consumption (from an average of 47 MVAr to 43 MVAr), an increase of the power factor (by 6% the average value) and an increase of the average active power (from 62 MW to 69 MW).

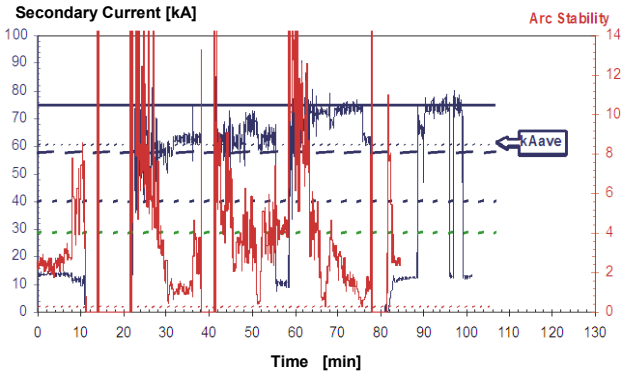

Fig. 6 Current in the secondary and electric arc's stability

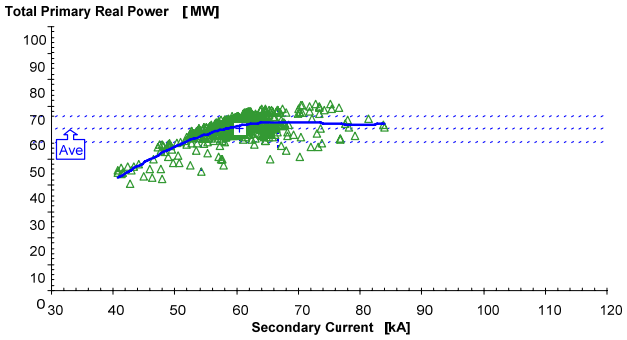

Fig. 7 The active power variation curve in the melting phase (early melt)

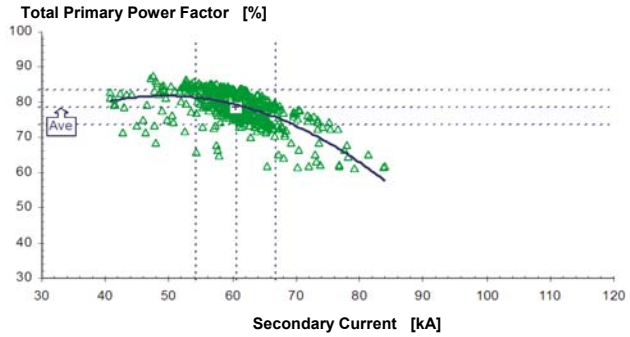

Fig. 8 The reactive power variation curve in the melting phase (early melt)

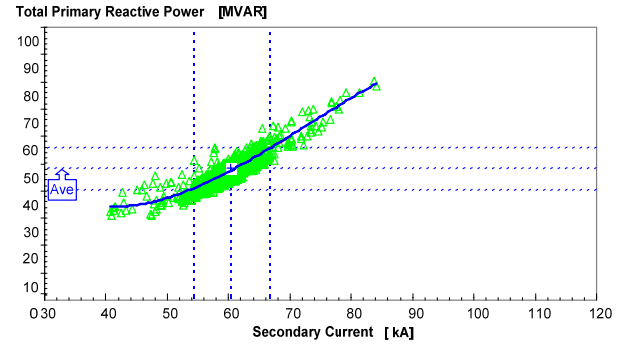

Fig. 9 Power factor in the EAF's primary (early melt)

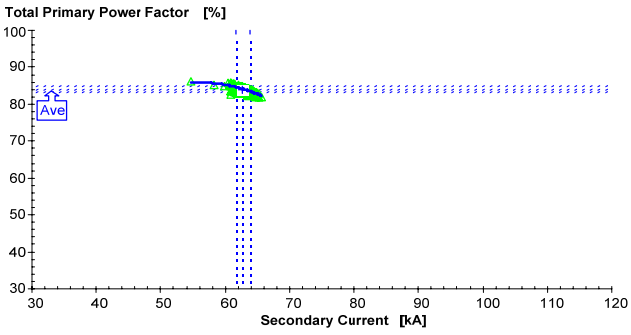

Fig. 10 Power factor in the EAF's primary (late melt)

The scope of study is to analyze the PF improve, identify operating parameters expected in the future, and evaluate [16]:

- EAF performance from the point of view of electrical energy with recommendations to improve;
- recommendations regarding the power factor problem (MVAR required, bank configuration, number of filters and tuning reactor specification);
- evaluate existing electrode regulator performance and point to improvement opportunities;
- recommend the best operating set-points to nun its EAF efficiently;
- identify operative characteristics and system restrictions in different heat stages.

4 Solution for EAF improvement performances

From the collected data analysis we can notice several possibilities for improvement: power factor compensation with passive elements (capacitors and inductive elements) or active compensation with SVC. Further, are presented the simulations results obtained with compensation with passive elements were considered four situations: one without series reactor (case R = 0) and three with series reactor having the resistances of 1, 2 and 3 ohm.

Currently, the variation of the absorbed power, the unbalance on phases, the flicker effect and the distorsion of the wave forms of the voltages and currents is not imputed to the consumer only by the reactive energy absorbed to a power factor smaller than the neutral one (Kp = 92%).

However, the modern norms will take into account all these aspects, and the operation costs with such unbalances will increase spectacularly. Therefore is necessary the thinking of some systems that should allow the alignment to the new standards.

In fig. 11 is presented a proposal of automatic system for compensation, filtration and balancing.

There were made the following notations:

- T_1, T_2 – power transformers (one active and one for spare);
- T_3 – EAF's transformer;
- T_4 – LMF's transformer;
- TC – current transformers;
- TT – voltage transformers;
- EAF – electric arc furnace for melting;
- LMF - electric arc furnace for treatment and alloying;
- E – electrodes;
- AB – adaption block;
- PLC – programmable logic controller for compensation, filtration and balancing;
- FBSH – filtration block for superior harmonics;

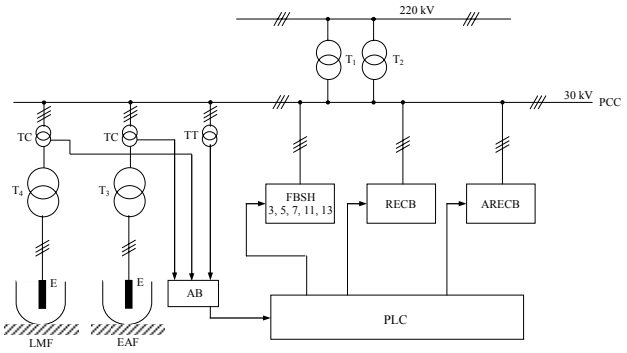

Fig. 11 Block diagram of the balancing and compensation system

- RECB – reactive energy compensation block with reactances of fixed capacity;
- ARECB – additional reactive energy compensation block and load balancing.

The PLC receives the current and voltage information from the current and voltage transformers, for each phase, by means of the adaption block. Based on the implemented management program, is controlled the harmonics filtration, respectively the compensation of the reactive energy and load balancing on phases. The harmonics' filtration block contains coils and capacitors tuned on the frequency corresponding to the harmonics 3, 5, 7, 11, 13 which in practice was found that they have a higher proportion.

Their connection or disconnection is made by static contactors controlled by the PLC.

The reactive energy's compensation block with fixed capacity reactances (RECB) is connected in circuit during the entire heat and, is calculated in such way that at the average value of the reactive energy on a heat to be achieved a neutral power factor. When the furnace is in stand-by, this block is disconnected.

The additional compensation block of the reactive energy (ARECB) introduces and takes out dynamically, at the command given by the PLC, by static contactors, batteries of capacitors for compensating the reactive energy that exceeds the average on a heat in such way that the power factor to not decrease under the neutral value. Also within this block there is the load balancing installation with coils and capacitors, which in real time introduces or takes out reactances from the circuit in such way that the distorsion factor of the currents respectively voltages to be under the permitted limits and the values of the phase differences between currents and between voltages to correspond to a symmetric system. In this block have plane important transitory phenomena. The state-of-the-art installations are using frequency converters that create a capacitive or inductive regime depending on the process requirement, instead of the ARECB block.

In table IV are presented the results of the simulations made for compensating the reactive energy by introducing of capacitor batteries with power between 20 MVAr and 50 MVAr. Is considered the case of compensation up to the power factor of 94%, taking into account the reactive energy consumptions in 2008 [16].

In the first case (Kp = 92%) a capacitor battery having 40 MVAr is sufficient for the entire reactive energy consumption and in the second case (Kp=94%) the value is of 45 MVAr (table IV).

In fig. 12, 13, 14, 15, 16 are presented the variation curves of the active power from the EAF transformer's primary with the current from the secondary for the actual case (fig. 12), for the case with capacitors battery without reactor (fig. 13) and for the case with capacitors battery and reactor with the resistance of 1, 2, 3 Ω (fig. 14, 15, 16).

Table IV

2008	Kp = 92%									Kp = 94%							
Month	Required Reactive Power [MVAr]	Equivalent Capacitor [kVAr]	Missing MVAr Compensation (-) Size of Capacitor Bank [kVAr]							Required Reactive Power [MVAr]	Equivalent Capacitor [kVAr]	Missing MVAr Compensation (-) Size of Capacitor Bank [kVAr]						
			20000	25000	30000	35000	40000	45000	50000			20000	25000	30000	35000	40000	45000	50000
1	11,566.34	34,790	-4,917	-3,255	-1,592	70	1,732	3,394	5,057	13,139.35	39,521	-6,490	-4,828	-3,166	-1,503	159	1,821	3,484
2	8,861.45	29,616	-2,877	-1,381	115	1,611	3,107	4,603	6,099	10,296.69	34,412	-4,312	-2,816	-1,320	176	1,672	3,168	4,664
3	12,702.78	38,208	-6,054	-4,391	-2,729	-1,067	596	2,258	3,920	14,220.59	42,774	-7,571	-5,909	-4,247	-2,584	-922	740	2,402
4	12,813.66	39,871	-6,386	-4,779	-3,172	-1,565	42	1,648	3,255	14,454.53	44,977	-8,027	-6,420	-4,813	-3,206	-1,599	8	1,614
5	11,196.41	33,677	-4,547	-2,885	-1,223	440	2,102	3,764	5,427	12,874.92	38,726	-6,226	-4,563	-2,901	-1,239	424	2,086	3,748
6	7,589.29	23,615	-1,162	445	2,052	3,659	5,266	6,873	8,480	8,758.96	27,254	-2,331	-724	882	2,489	4,096	5,703	7,310
7	9,538.67	28,691	-2,889	-1,227	435	2,097	3,760	5,422	7,084	10,902.72	32,794	-4,253	-2,591	-929	733	2,396	4,058	5,720
8	8,119.01	24,421	-1,470	193	1,855	3,517	5,179	6,842	8,504	9,339.23	28,091	-2,690	-1,028	635	2,297	3,959	5,622	7,284
9	8,611.14	26,794	-2,184	-577	1,030	2,637	4,244	5,851	7,458	9,924.90	30,882	-3,497	-1,890	-284	1,323	2,930	4,537	6,144
10	12,182.64	36,644	-5,533	-3,871	-2,209	-546	1,116	2,778	4,440	13,920.91	41,872	-7,272	-5,609	-3,947	-2,285	-622	1,040	2,702
11	10,091.32	31,400	-3,664	-2,057	-450	1,157	2,764	4,371	5,978	11,491.33	35,756	-5,064	-3,457	-1,850	-243	1,364	2,971	4,578
12	10,297.52	31,612	-3,789	-2,162	-535	1,092	2,719	4,346	5,973	11,756.74	36,096	-5,249	-3,622	-1,994	-367	1,260	2,887	4,514

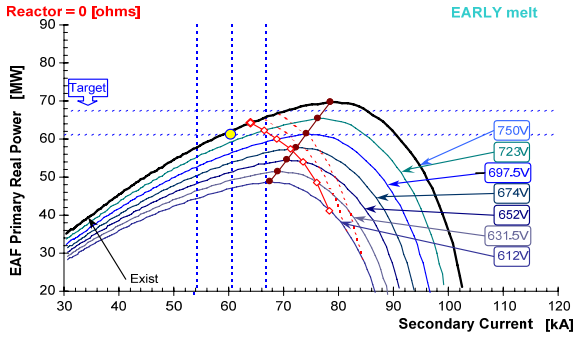

Fig. 12 Variation curves of the active power without capacitors battery and without reactor (R=0 Ω)

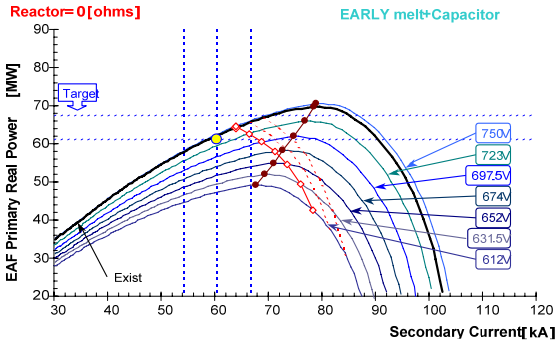

Fig. 13 Variation curves of the active power with capacitors battery and without reactor (R = 0 Ω)

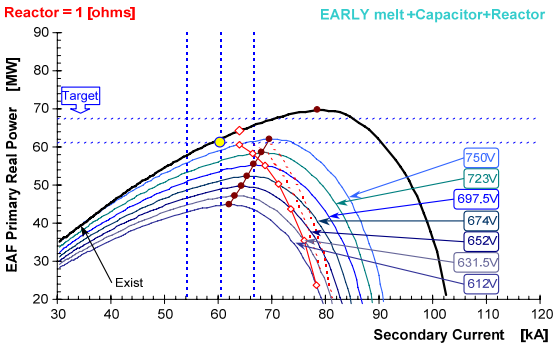

Fig. 14 Variation curves of the active power with capacitors battery and reactor (R = 1 Ω)

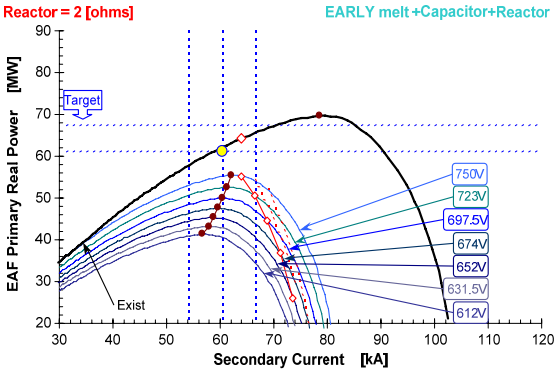

Fig. 15 Variation curves of the active power with capacitors battery and reactor (R = 2 Ω)

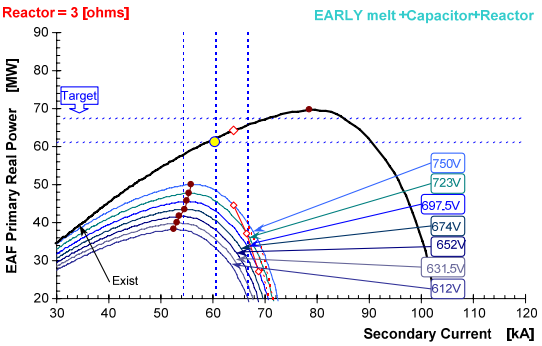

Fig. 16 Variation curves of the active power with capacitors battery and reactor (R = 3 Ω)

One can notice that the available active power at a certain current through the electric arc is more smaller as the voltage in secondary is smaller and the reactor's resistance is higher.

The average capacitor requirement at 30kV to fit 94% power factor are 36.1 MVAr at early melt and 30.5 MVAr at late melt. Recommended size is 45 MVAr at 30kV, providing more than 94% power factor compensation. It is recommended to use the complete 45 MVAr in one filter tuned on the 3rd harmonic order (about 2.9, depending upon resonance conditions).

The modernization work is in progress and no solution was finally considered.

6 Conclusion

In this paper, the 100t Electric Arc Furnace (EAF) for steel production is analyzed. The flicker mitigation and reactive power compensation requirements are quantitatively analyzed. The various compensation solutions are compared, such as, passive filter, SVC, and STATCOM.

Supplementary series reactors are widely used in high power AC EAF to allow furnace operation with longer arcs, lower currents and lower electrode consumption. Such reactors can be switched off in the final stages of the melting process, when the electric arc is stable and arc ignition is not of great concern.

A menu for optimum operation of the EAF system should be prepared in terms of EAF transformer and series reactor taps and electrode current settings for different phases of the melting process.

Using the compensation of reactive energy, harmonic filtering and load balancing determines the increase of the power factor more than neutral value (92%), reduction of the harmonic emission in the electric grid, reduction flicker and deforming effect on the grid.

References:

[1] S.I. Deaconu, M. Topor, G.N. Popa, I. Popa, "Comprehensive Analysis for Modernization of 100 t Electric Arc Furnace for Steel Production", IAS 2009, *44th Annual Meeting*, Houston, Texas, SUA, CFP 09 IAS-CDR, ISBN 978-1-4244-3476-3, pp. 143-148.

[2] ***, "Globalization and Consolidation in the Steel Industry", *Joint India/OECD/IISI Workshop*, New Delhi, 16-17 May 2006, p.17 (http://steel.nic.in/oecd/DSTI_SU_SC(2006)7_ ENG.pdf).

[3] S. R. Mendis, M. T. Bishop, and J. F. Witte, "Investigations of Voltage Flicker in Electric Arc Furnace Power Systems", *IEEE Industry Applications Magazine*, January/February, 1996, pp. 28-34.

[4] I. Vervenne, K. Van Reusel, and R. Belmans, " Electric Arc Furnace Modeling from a Power Quality Point of View", *9th International Conference Electrical Power Quality and Utilization*, Barcelona, 9-11 October 2007.

[5] P. Ashmole and P. Amante, "System flicker disturbances from industrial loads and their compensation" Power Eng. J., vol. 11, no. 5, pp. 213-218, October, 1997.

[6] M. Routimo, D.J. Carnavale, "Capacitor Application Issues," IEEE Transactions on Industry Applications, vol. 44, no. 4, pp. 1013-1026, July/August, 2008.

[7] J. J. Trageser , "Power Usage and Electrical Circuit Analysis for Electric Arc Furnaces" , IEEE Transaction on Industry Application, Vol. IA-16, no. 2, March/April 1980 , pp.277-284.

[8] M. Pănoiu, C. Pănoiu, I. Şora, "Modeling the electromagnetic pollution of the electric arc furnaces", Rev. Roum. Sci. Techn. – Électrotechn. et Énerg., 54, *2*, pp. 165–174, Bucharest, 2009.

[9] M. Pănoiu , C. Pănoiu , I. Şora , R. Rob ,"Using simulation for study the Posibility of Canceling Load Unbalance of non-sinusoidal High Power three-phase Loads" , WSEAS Transactions on Systems , Issue 7 , Volume 7, July 2008 , ISSN 1109-2777 , pp 699-710.

[10] G.O.Tirian , C. Bretotean Pinca ,"Applications of Neural Networks in Continuous Casting", WSEAS Transactions on Systems , Issue 6 , Volume 8, June 2009 , ISSN 1109-2777 , pp 693-702.

[11] M. Pănoiu, C. Pănoiu, I. Şora, R. Rob, "Simulation of the flicker Phenomenon based on Modeling the Electric Arc ", WSEAS Transactions on Systems, Issue 10, Volume 7, October 2008, ISSN 1109-2777, pp 1132-1142.

[12] C. Han, A.Q. Huang, S. Bhattacharya, L.W. White, M. Ingram, S. Atcitty and W. Wong, "Design of an Ultra-capacitor Energy Storage Systems (UESS) for POWER Quality Improvement of Electric Arc Furnaces", IAS 2008, ISBN 978-1-4244-2279-1, 6 pp.

[13] C. Han, A.Q. Huang, S. Bhattacharya and M. Ingram, "Field Data-base Study on Electric Arc Furnace Flicker Mitigation", IAS 2006, ISBN 978-1-4244-0365-0, 6 pp.

[14] X. Yang , J. Zhao , J. Jiang ,"An improved dc capacitor voltage detection technology and its FPGA implementation in the CHB-based STATCOM", WSEAS Transactions on Systems, Issue 1 , Volume 9, October 2010, ISSN 1109-2777 , pp 20-30.

[15] A. Iagăr, G.N. Popa, I. Şora, "Analysis of Electromagnetic Pollution Produced by Line Frequency Coreless Induction Furnaces", WSEAS Transactions on Systems, Issue 1, Volume 8, January 2009, ISSN 1109-2777, pp 1-11.

[16] A. Mariscal, AMI GE, Report no.A1360, 2006 (unpublished).

[17] C.M. Diniş, G.N. Popa, A. Iagăr," Mathematical Modeling and Simulation in Matlab/Simulink of Processes from Iron Ore Sintering Plants", WSEAS Transactions on Systems, Issue 1, Volume 8, January 2009, ISSN 1109-2777 , pp 34-43.